

Understanding the Geometry of Dynamics: Invariant Manifolds and their Interactions

Hinke M. Osinga

Department of Mathematics, University of Auckland, Auckland, New Zealand

Abstract

Dynamical systems theory studies the behaviour of time-dependent processes. For example, simulation of a weather model, starting from weather conditions known today, gives information about the weather tomorrow or a few days in advance. Dynamical systems theory helps to explain the uncertainties in those predictions, or why it is pretty much impossible to forecast the weather more than a week ahead. In fact, dynamical systems theory is a geometric subject: it seeks to identify critical boundaries and appropriate parameter ranges for which certain behaviour can be observed. The beauty of the theory lies in the fact that one can determine and prove many characteristics of such boundaries called invariant manifolds. These are objects that typically do not have explicit mathematical expressions and must be found with advanced numerical techniques. This paper reviews recent developments and illustrates how numerical methods for dynamical systems can stimulate novel theoretical advances in the field.

1 Introduction

Mathematical models in the form of systems of ordinary differential equations arise in numerous areas of science and engineering—including laser physics, chemical reaction dynamics, cell modelling and control engineering, to name but a few; see, for example, [12, 14, 35] as entry points into the extensive literature. Such models are used to help understand how different types of behaviour arise under a variety of external or intrinsic influences, and also when system parameters are changed; examples include finding the bursting threshold for neurons, determining the structural stability limit of a building in an earthquake, or characterising the onset of synchronisation for a pair of coupled lasers. In fact, the investigation of a specific mathematical model is not only of great use for explaining observed behaviour in the application context, but it also allows one to identify general or typical features that must be expected to occur in any system, under mild assumptions on the equations and their dependence on system parameters.

The theory of dynamical systems describes such “universal” geometric features of behaviour, which comprise a language that has proven extraordinarily useful in the analysis of dynamical models across the sciences: it effectively tells one what to expect and what to look for in a given system. The theory is inherently geometric in nature, in that it requires one to understand the overall organisation of phase space by (hyper)surfaces known as global invariant manifolds, which are associated with objects such as saddle equilibria (rest-state behaviour) and periodic orbits (oscillatory behaviour). In short, the interactions of invariant manifolds

determine the overall behaviour, and they are the key to understanding the geometry of the observed dynamics. This point of view was introduced by Poincaré to demonstrate instabilities of planetary motion [4, 36]. Similar geometric arguments were used in the 1970s to show that the famous Lorenz system features chaotic dynamics and unpredictability [16, 25]. This geometric theory has benefited enormously from the progress in scientific computing and the recent development of numerical methods that allow one to find invariant manifolds, and to investigate their interactions and bifurcations as parameters are changed [15, 23, 24]. Numerical approximations have yielded new insights into the overall organisation of phase space in the transition to chaos [9, 10], near certain types of global bifurcations and singularities [2, 3], and as mechanisms for so-called mixed-mode oscillations (MMOs) [7, 8].

This paper explains how recently developed numerical methods for dynamical systems can be used to stimulate novel theoretical advances in the field. We focus on the Lorenz system [25] as a classical example of a dynamical system that exhibits unpredictable and surprisingly complicated behaviour. We first introduce the relevant invariant manifolds, including the so-called Lorenz manifold, which is a very intriguing surface. We compute these manifolds and show how they organise the observed dynamics. In particular, we present and illustrate the amazing structure of the Lorenz manifold and discuss the consequences for the overall organisation of phase space. We end with a brief conclusion section.

2 The Lorenz system

The Lorenz system is given by the following system of three ordinary differential equations:

$$\begin{cases} \dot{x} &= \sigma(y - x), \\ \dot{y} &= \rho x - y - xz, \\ \dot{z} &= xy - \beta z, \end{cases} \quad (1)$$

where $\sigma = 10$, $\rho = 28$ and $\beta = 8/3$. Such a system is also called a vector field or force field, because the right-hand side defines a velocity vector and each point (x_0, y_0, z_0) in phase space experiences a force that pushes it in the direction of the velocity vector with the speed determined by the length of that vector. Solutions of system (1) are called trajectories. A trajectory through a particular point (x_0, y_0, z_0) is given by the solution of (1) that passes through (x_0, y_0, z_0) , that is, it is given by the set

$$\{\Phi_t(x_0, y_0, z_0) \in \mathbb{R}^3 \mid t \in \mathbb{R}\},$$

where Φ is the evolution operator or flow associated with system (1).

The Lorenz system is a classical example of a dynamical system that exhibits sensitive dependence on initial conditions. This means that the trajectories starting from any two points that lie arbitrarily close to each other will move apart so dramatically, that it is impossible to verify after a reasonably short period of time whether the two trajectories were ever close to each other. Lorenz [25] derived his example as a much simplified model of convection in the atmosphere. The standard parameter values $\sigma = 10$, $\rho = 28$ and $\beta = 8/3$ are the ones provided by Lorenz as a relatively realistic choice. For these parameter values, all trajectories will converge quickly to a strange attracting object, known as the butterfly attractor or Lorenz attractor, which occupies only a small part of the phase space \mathbb{R}^3 . Hence, most studies in the literature have focussed on explaining the behaviour of the system on the Lorenz attractor. Geometrically, the Lorenz attractor is a rather intriguing object: it is larger than a one-dimensional

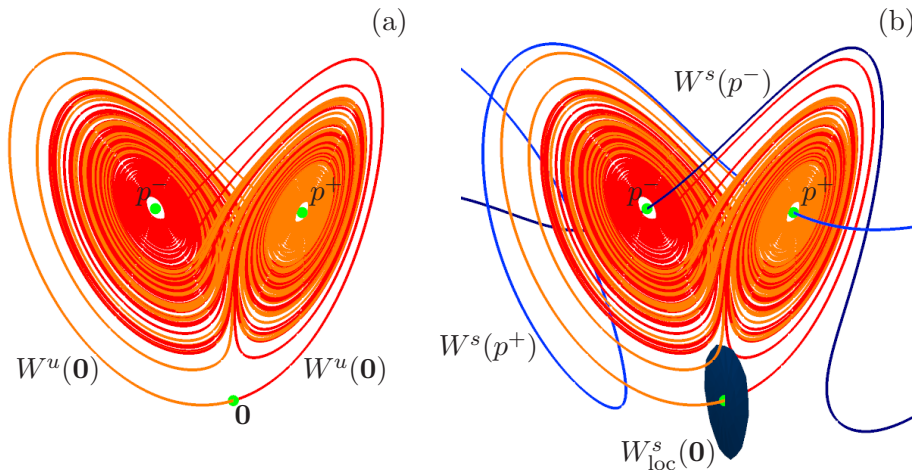


Figure 1: The strange attractor of the Lorenz system (1) is represented in panel (a) by the one-dimensional unstable manifold $W^u(\mathbf{0})$ of the equilibrium $\mathbf{0}$; panel (b) illustrates part of the skeleton of the Lorenz system, which also includes the equilibria p^\pm , their one-dimensional stable manifolds $W^s(p^\pm)$ and the two-dimensional local stable manifold $W^s_{\text{loc}}(\mathbf{0})$.

curve, or even set of curves, but it is not a two-dimensional object; mathematically, such an attractor is called a *strange attractor*.

Figure 1(a) gives an impression of the Lorenz attractor. It shows two trajectories on the attractor; they both have the special property that they converge to the origin $\mathbf{0}$ in backward time. Indeed, $\mathbf{0}$ is an equilibrium (steady state) of system (1), but it is of saddle type, that is, it is neither attracting in forward nor in backward time. Hence, the two trajectories are indeed quite special. In fact, they are the only two trajectories that converge to $\mathbf{0}$ in backward time, and together, they form what is known as the unstable manifold $W^u(\mathbf{0})$ of $\mathbf{0}$. In forward time, the two trajectories oscillate around two other equilibria, denoted p^\pm , which are related by rotational symmetry over 180 degrees about the (vertical) z -axis. In the analogy of the butterfly attractor, the equilibria p^\pm lie at the centre of its ‘wings’ and trajectories move irregularly from one wing of the butterfly to the other. The Lorenz attractor is composed of more than just two trajectories; it consists of infinitely many trajectories. Nevertheless, it is generally believed that the Lorenz attractor is equal to the *closure* of $W^u(\mathbf{0})$ [34]. This means that it consists of $W^u(\mathbf{0})$ and the limit points of all arbitrary sequences of points in $W^u(\mathbf{0})$.

2.1 Stable Manifold Theorem and the skeleton

It is not hard to show that the three equilibria $\mathbf{0}$ and p^\pm are the only equilibria of (1); the coordinates of p^\pm are

$$\begin{aligned}
 p^+ &= \left(\sqrt{\beta(\varrho - 1)}, \sqrt{\beta(\varrho - 1)}, \varrho - 1 \right) \approx (8.4853, 8.4853, 27), \quad \text{and} \\
 p^- &= \left(-\sqrt{\beta(\varrho - 1)}, -\sqrt{\beta(\varrho - 1)}, \varrho - 1 \right) \approx (-8.4853, -8.4853, 27).
 \end{aligned}$$

Their stability is determined by the eigenvalues of the Jacobian matrix (of partial derivatives of the right-hand side) evaluated at the respective equilibrium point. If all eigenvalues lie in the left half of the complex plane then the equilibrium is stable; if at least one eigenvalue is

positive, or there exists a pair of complex-conjugate eigenvalues with positive real part, then the equilibrium is unstable. For $\mathbf{0}$, we find that the eigenvalues are

$$-\beta \quad \text{and} \quad -\frac{\sigma+1}{2} \pm \frac{1}{2}\sqrt{(\sigma+1)^2 + 4\sigma(\rho-1)},$$

that is, there are two stable eigenvalues $-8/3$ and $-5\frac{1}{5} - \frac{1}{2}\sqrt{1201} \approx -22.8277$ and one unstable eigenvalue $-5\frac{1}{5} + \frac{1}{2}\sqrt{1201} \approx 11.8277$. Similarly, p^+ has one stable eigenvalue and a complex-conjugate pair of unstable eigenvalues; the approximate values are -13.8546 and $0.0940 \pm 10.1945i$. Due to the rotational symmetry, p^- has exactly the same eigenvalues as p^+ .

We conclude that all equilibria are of saddle type, because they have both stable and unstable eigenvalues. Then the *Stable Manifold Theorem* guarantees that there exist stable and unstable manifolds associated with each of the saddle equilibria that have the same dimensions as the number of stable and unstable eigenvalues, respectively [31]; furthermore, the eigenspaces associated with these eigenvalues are tangent to the corresponding manifolds at the equilibrium. For example, the unstable manifold $W^u(\mathbf{0})$ consists of all trajectories that converge to $\mathbf{0}$ in backward time. It is formally defined as

$$W^u(\mathbf{0}) = \{(x_0, y_0, z_0) \mid \lim_{t \rightarrow -\infty} \Phi_t(x_0, y_0, z_0) = \mathbf{0}\}.$$

We already mentioned that $W^u(\mathbf{0})$ consists of only two trajectories. Indeed, since $\mathbf{0}$ has only one unstable eigenvalue, its unstable manifold is one-dimensional curve. Similarly, its stable manifold $W^s(\mathbf{0})$ consists of all trajectories that converge to $\mathbf{0}$ in forward time, or

$$W^s(\mathbf{0}) = \{(x_0, y_0, z_0) \mid \lim_{t \rightarrow \infty} \Phi_t(x_0, y_0, z_0) = \mathbf{0}\}.$$

The origin $\mathbf{0}$ has two stable eigenvalues and $W^s(\mathbf{0})$ is, thus, a two-dimensional surface.

Together, the equilibria and their invariant manifolds form the so-called skeleton of the Lorenz system. This is illustrated in panel (b) of Figure 1. This figure shows only a small first (local) part of $W^s(\mathbf{0})$, which is denoted $W_{\text{loc}}^s(\mathbf{0})$ in the figure. Also shown are the two symmetrically-related one-dimensional stable manifolds $W^s(p^\pm)$ of p^\pm , which each consist of the only two trajectories that converge to p^+ or p^- in forward time.

Stable and unstable manifolds are not easy to find, not even when they are one dimensional. This is because it is usually not possible to find an explicit expression for solutions to the system of differential equations. Hence, (un)stable manifolds are only defined in the above abstract and implicit sense by the properties of the solutions contained in them. Therefore, (un)stable manifolds can generally only be found by numerical approximation. The computation of one-dimensional (un)stable manifolds, such as those in Figure 1, is relatively easy, because it involves numerical approximation of only two trajectories, which can be found by numerical integration of the system of equations. However, a two-dimensional (un)stable manifold comprises infinitely many trajectories!

2.2 The Lorenz manifold

The two-dimensional stable manifold $W^s(\mathbf{0})$ of the Lorenz system (1) is particularly challenging to compute, because of extreme local and global stretching associated with the chaotic dynamics. This means that it is very difficult to design an algorithm that generates a high-quality mesh on the surface. Figure 2 shows a first part of the global manifold $W^s(\mathbf{0})$. It was computed

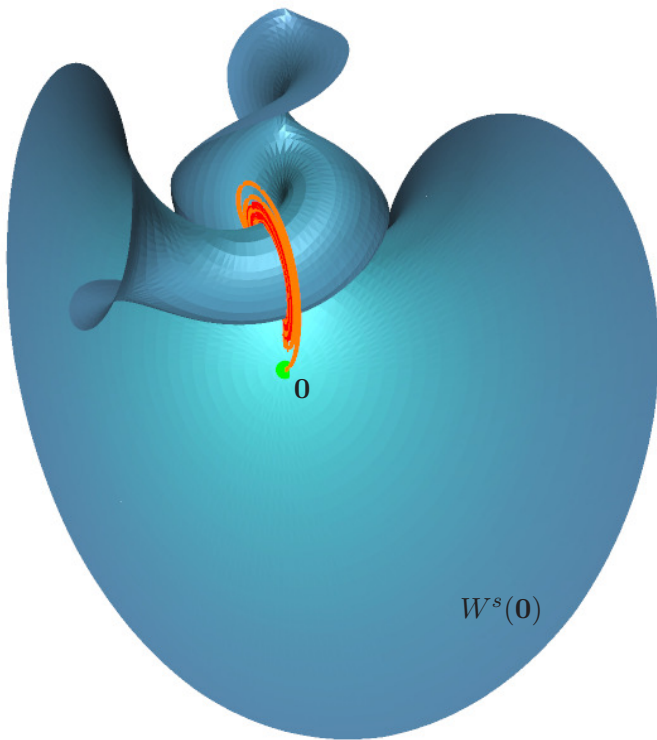


Figure 2: The two-dimensional stable manifold $W^s(\mathbf{0})$ of the Lorenz system (1), shown together with the one-dimensional unstable manifold $W^u(\mathbf{0})$; the image shows $W^s(\mathbf{0})$ up to geodesic distance 100.

with the method presented in [21, 22], which approximates the surface as a collection of concentric closed curves that are level sets of the function that measures geodesic distance to $\mathbf{0}$ along $W^s(\mathbf{0})$. The survey paper [24] discusses other common algorithms, and all contributors use $W^s(\mathbf{0})$ as the test-case example to illustrate their numerical approach; it is in this publication that $W^s(\mathbf{0})$ has been given the name *Lorenz manifold*.

Stable and unstable manifolds play an important role in organising the behaviour of a dynamical systems. We already saw that $W^u(\mathbf{0})$ gives information about the strange attractor of the Lorenz system (1). The stable manifold of the Lorenz system (1) is perhaps even more important: it gives information about the overall organisation of chaos in the Lorenz system throughout the entire three-dimensional phase space.

The Lorenz manifold is a complicated surface. Since it only consists of trajectories that converge to $\mathbf{0}$, it cannot contain the trajectories that converge to p^+ or p^- , that is, it does not contain p^\pm and $W^s(p^\pm)$. Furthermore, for the classical parameter values, there is no trajectory that converges to $\mathbf{0}$ in both forward and backward time, which means that $W^s(\mathbf{0})$ also does not contain $W^u(\mathbf{0})$. Hence, the surface wraps around these one-dimensional curves and intersects neither $W^s(p^\pm)$ nor $W^u(\mathbf{0})$. As a consequence, $W^s(\mathbf{0})$ forms a helical shape near the positive z -axis. In fact, $W^s(\mathbf{0})$ contains the z -axis: the trajectory through an initial condition of the form $(0, 0, z_0)$ is known explicitly as the vertical line $\{(0, 0, z(t)) \mid z(t) = z_0 e^{-\beta t}\}$, which converges to $\mathbf{0}$ in forward time, because $-\beta = -8/3 < 0$. Moreover, $W^s(\mathbf{0})$ is itself symmetric under rotation by 180 degrees around the z -axis. The numerical study of $W^s(\mathbf{0})$ in [24] shows that the Lorenz manifold contains additional helices very close to the z -axis, formed in symmetric pairs. Further away from the z -axis, $W^s(\mathbf{0})$ wraps around $W^s(p^\pm)$. Figure 2 shows only one

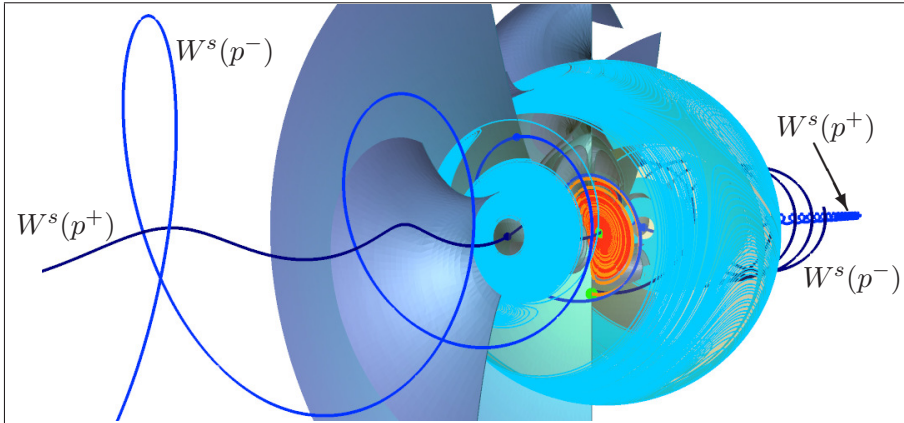


Figure 3: Intersection curves of $W^s(\mathbf{0})$ with the sphere S_R . Also shown are the skeleton from Figure 1(b), with $W^s(p^\pm)$ computed up to a much longer arclength.

such wrapping, but each half twist up the helix leads to a wrap around $W^s(p^\pm)$ as well.

2.3 The geometry of the Lorenz manifold

In the past decade efforts have shifted from the challenge of computing the Lorenz manifold to that of understanding its geometry. We view the Lorenz manifold as a key object for understanding how the chaotic dynamics manifests itself globally in the Lorenz system (1). Its properties reflect the presence of sensitive dependence on initial conditions, which is present not only on the Lorenz attractor, but also everywhere else in phase space. Since the Lorenz attractor is a global attractor, any two points that lie close together will first flow quickly to the Lorenz attractor and start a pattern of oscillations around p^+ and p^- ; initially these oscillations will be around the same equilibrium, but after some time one of the trajectories will switch to oscillate, say, around p^- , while the other makes one more turn around p^+ . From then on their switches between oscillations around p^+ and p^- will be completely different. This switching is controlled by $W^s(\mathbf{0})$: a trajectory cannot cross $W^s(\mathbf{0})$ and it can only change its centre of oscillation by following one of the many wrapping layers of $W^s(\mathbf{0})$ from p^\pm to p^\mp . This means that the global invariant manifold $W^s(\mathbf{0})$ separates practically any two points in \mathbb{R}^3 , even if they lie arbitrarily close together. Mathematically, this means that $W^s(\mathbf{0})$ is *dense* in \mathbb{R}^3 , that is, this two-dimensional smooth surface fills the entire three-dimensional space.

The Lorenz manifold is the first known example of a space-filling surface realised by a dynamical system [11]. Because of the dimensions involved, it is not easy to visualise this topological property. The following idea was introduced in [10, 11]: rather than studying the entire phase space, consider only the intersection curves of $W^s(\mathbf{0})$ with a suitably large sphere, which we denote S_R . It turns out that the properties of $W^s(\mathbf{0})$ are best visualised if S_R surrounds the Lorenz attractor entirely, that is, if $W^u(\mathbf{0})$ is inside and never intersects the sphere S_R . Therefore, we choose the mid-point on the line segment between p^\pm , that is, the point $(0, 0, 27)$ as the centre of S_R . Hence, its radius R must be at least 27. For technical reasons, we choose $R = 70.7099$, which is quite a bit larger; for details on this particular choice, see [11].

It is important to realise that S_R is compact and bounded. The intersection set $\widehat{W^s(\mathbf{0})}$ of $W^s(\mathbf{0})$ with S_R consists of either closed curves or spiralling curves that accumulate, at both

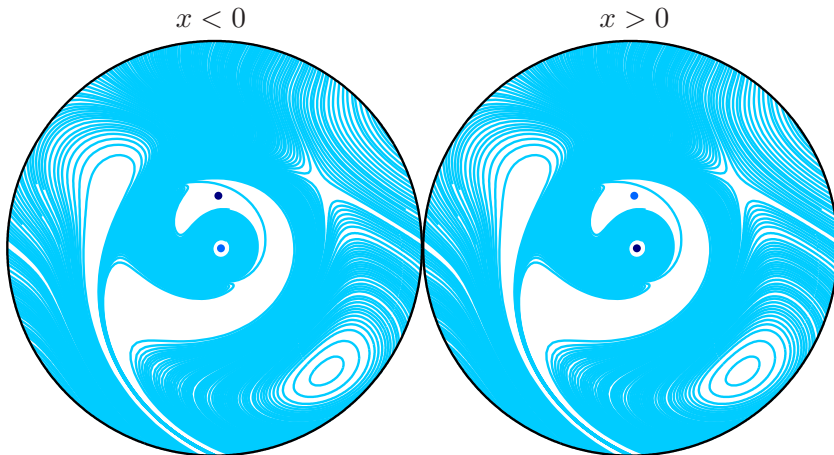


Figure 4: Stereographic projection of the computed intersection curves in $\widehat{W}^s(\mathbf{0})$.

ends, onto a point or (closed) curve. We already know that $W^s(\mathbf{0})$ wraps around $W^s(p^\pm)$, so we expect that the intersection curves with S_R will spiral around the four points where two pairs of branches of $W^s(p^\pm)$ intersect S_R . Furthermore, since $W^s(\mathbf{0})$ is a space-filling surface, we must have that the intersection curves in $\widehat{W}^s(\mathbf{0})$ densely fill S_R . Figure 3 illustrates how $W^s(\mathbf{0})$ intersects the sphere S_R . Here, the surface of $W^s(\mathbf{0})$ was calculated up to a much larger geodesic distance. A separate computational method was used to find even more curves in $\widehat{W}^s(\mathbf{0})$ directly. Furthermore, $W^s(\mathbf{0})$ is sliced in two and only the half with negative y -coordinates is rendered in Figure 3. The sphere S_R is transparent, so one can see $\mathbf{0}$ and $W^u(\mathbf{0})$ inside, as well as p^+ (p^- is obscured in the figure). There are two (blue) curves intersecting S_R in the half with positive x -coordinate; the darker-blue curve is one of the trajectories from $W^s(p^+)$ and the lighter-blue one is from $W^s(p^-)$; the symmetrically opposite trajectories in $W^s(p^+)$ and $W^s(p^-)$ can be seen disappearing in the background as the lighter-blue and darker-blue curves, respectively. The many intersection curves in $\widehat{W}^s(\mathbf{0})$ on S_R are coloured cyan.

We now consider just the sphere S_R with the intersections set $\widehat{W}^s(\mathbf{0})$ and the four intersections points of $W^s(p^\pm)$ with S_R . We use the technique called *stereographic projection* to represent one half of S_R by a flat disk. Figure 4 shows the two projections along the negative and positive x -axes. The boundary of the disk is the equator with $x = 0$, and the two disks touch at the point that corresponds to $(0, 70.7099, 0)$ on S_R . By rolling, say, the left disk along the rim of the right disk, we can see how curves on one disk continue smoothly onto the other disk, meaning that a curve in the half-sphere with $x > 0$ crosses the equator $x = 0$ and continues onto the other half of S_R . Due to the rotational symmetry of system (1), the intersection set $\widehat{W}^s(\mathbf{0})$ of the Lorenz manifold is exactly the same on the two half-spheres. Note that this symmetry exchanges the intersection sets of the manifolds $W^s(p^\pm)$. More precisely, the dark-blue dot that lies approximately in the centre of the half-sphere with $x > 0$ (right) is the intersection point of the dark-blue trajectory in $W^s(p^+)$ coming towards you in Figure 3.

Figure 4 shows a large number of the infinitely many intersection curves in $\widehat{W}^s(\mathbf{0})$. Of course, it is only possible to compute finitely many of these intersection curves. Nevertheless, our computational approach provides further insight into how $\widehat{W}^s(\mathbf{0})$ fills S_R . We fix a maximum total integration time T_{\max} and computes all those intersections curves associated with trajectories that flow from S_R to $\mathbf{0}$ and reach the small first (local) part $W_{\text{loc}}^s(\mathbf{0})$ in at most this maximum time T_{\max} ; details can be found in [11]. By increasing the choice for T_{\max} from

the moment that intersection curves appear on S_R , we can follow the process of how further intersection curves are added as the integration time increases. It turns out that there is a very specific order in which the intersection curves emerge. They grow in an exponential fashion with curves appearing in ever increasing numbers; furthermore, the locations where new curves appear lie in between previously computed curves in a very ordered way. This process of adding curves in particular locations gives rise to a so-called Cantor structure, and $\widehat{W}^s(\mathbf{0})$ is locally a Cantor set of curves; see also [10, 30].

The nature of $\widehat{W}^s(\mathbf{0})$ on S_R reflects the geometry of $W^s(\mathbf{0})$ in the three-dimensional phase space. However, $W^s(\mathbf{0})$ is a single smooth surface! The many layers of $W^s(\mathbf{0})$ that wrap around $W^s(p^\pm)$ are responsible for creating the infinitely many intersection curves in $\widehat{W}^s(\mathbf{0})$, which means that $W^s(\mathbf{0})$ has infinitely many layers that wrap around $W^s(p^\pm)$, and they do so in a very complicated but systematic fashion; indeed, our observations of how $\widehat{W}^s(\mathbf{0})$ fills S_R tell us how intricate the layering of $W^s(\mathbf{0})$ is. This is directly related to the sensitive dependence on initial conditions for the Lorenz system (1).

Note that the unfilled regions on the sphere S_R in Figure 3 and, correspondingly, on the disks shown in Figure 4, are due to the finite nature of the numerical computation. Trajectories on $W^s(\mathbf{0})$ that start in one of the unfilled region need integration times that are larger than T_{\max} before reaching $W_{\text{loc}}^s(\mathbf{0})$. Consequently, two such trajectories that start close together will take a comparatively large time to separate, indicating that the sensitivity in the dependence on initial conditions actually varies over different regions in phase space. Eventually, these regions will also be filled with intersection curves, but at the cost of increasing T_{\max} quite dramatically.

3 Conclusion

It is mind-boggling to realise that such innocent-looking equations as the Lorenz system (1) give rise to a two-dimensional smooth surface that lies dense in its three-dimensional phase space! One could ask how typical this property is. In fact, for the Lorenz system it is typical, in the sense that a small variation of the parameters σ , ρ and β will give an ever so slightly different Lorenz manifold, but it will still lie dense in \mathbb{R}^3 . However, this denseness property may change dramatically if the parameters are varied more than just a little. Concretely, for small $\rho > 0$ (less than 13.9265, to be precise), there is no chaotic dynamics. The Lorenz manifold for such small ρ -values does not fill \mathbb{R}^3 at all, but rather is a relatively simple surface that divides the phase space into the basins of the two equilibria p^\pm , which are now attractors. Its corresponding intersection set with the sphere S_R is a single closed curve for this case! Hence, the geometric properties of the Lorenz manifold for small ρ are completely different from those for $\rho = 28$.

The transition that turns the Lorenz manifold from a simple surface into a densely filling surface is a fascinating process that has been studied in detail in [10]; see also [1, 9, 18, 19, 20, 26, 27, 28, 32, 33, 34]. Our contributions to this study are based on sophisticated, efficient and highly accurate numerical methods that allow for detailed mathematical observations. More precisely, our findings provide detailed geometrical and topological insight into how Lorenz manifold and the overall dynamics of the Lorenz system changes in the transition from simple to chaotic dynamics. The numerical investigation of the Lorenz system and the Lorenz manifold, especially for values of ρ beyond $\rho = 28$, is ongoing research; the most recent developments can be found in [5, 6, 11].

The Lorenz system is an exciting example of a dynamical system that exhibits chaotic dynamics, but it is somewhat removed from the original physical motivation of describing convection in the atmosphere. However, it is of fundamental importance to the theory of dynamical systems as a hallmark and prototypical example of a chaotic system. Moreover, it is an excellent test case to demonstrate, more generally, what can be achieved with advanced methods. We believe that our computational methods for the computation of invariant manifolds have reached such a maturity that detailed mathematical statements can be made about the overall organisation of phase space. Indeed, other more realistic models from applications can be studied in the same spirit; for example, these methods have been applied recently to explain the spiking behaviour of neuronal cells [13, 29] and complicated oscillations in chemical reactions [17].

Acknowledgements

This paper reviews research in collaboration with other colleagues and especially with Bernd Krauskopf, who I also thank for comments on an earlier draft of this manuscript. My research is supported by Marsden Fund grant # 16-UOA-286.

References

- [1] Aguirre P, Doedel EJ, Krauskopf B, Osinga HM. 2011. Investigating the consequences of global bifurcations for two-dimensional invariant manifolds of vector fields. *Discrete and Continuous Dynamical Systems–Series A* **29**(4):1309–1344.
- [2] Aguirre P, Krauskopf B, Osinga HM. 2013. Global invariant manifolds near homoclinic orbits to a real saddle: (non)orientability and flip bifurcation. *SIAM Journal on Applied Dynamical Systems* **12**(4):1803–1846.
- [3] Aguirre P, Krauskopf B, Osinga HM. 2014. Global invariant manifolds near a Shilnikov homoclinic bifurcation. *Journal of Computational Dynamics* **1**(1):1–38.
- [4] Barrow-Green J. 1997. *Poincaré and the three-body problem*. American Mathematical Society, Providence (RI).
- [5] Creaser JL, Krauskopf B, Osinga HM. 2015. α -flips in the Lorenz system. *Nonlinearity* **28**(3):R39–R65.
- [6] Creaser JL, Krauskopf B, Osinga HM. Forthcoming. Finding first foliation tangencies in the Lorenz system. *SIAM Journal on Applied Dynamical Systems*.
- [7] Desroches M, Guckenheimer J, Krauskopf B, Kuehn C, Osinga HM, Wechselberger M. 2012. Mixed-mode oscillations with multiple time scales. *SIAM Review* **54**(2):211–288.
- [8] Desroches M, Krauskopf B, Osinga HM, 2009. The geometry of mixed-mode oscillations in the Olsen model for peroxidase-oxidase reaction. *Discrete and Continuous Dynamical Systems–Series S* **2**(4):807–827.
- [9] Doedel EJ, Krauskopf B, Osinga HM. 2006. Global bifurcations of the Lorenz manifold. *Nonlinearity* **19**(12):2947–2972.

- [10] Doedel EJ, Krauskopf B, Osinga HM. 2011. Global invariant manifolds in the transition to preturbulence in the Lorenz system. *Indagationes Mathematicae* **22**(3–4):222–240.
- [11] Doedel EJ, Krauskopf B, Osinga HM. 2015. Global organization of phase space in the transition to chaos in the Lorenz system. *Nonlinearity* **28**(11):R113–R139; with multimedia supplement.
- [12] Ermentrout GB, Terman DH. 2010. *Mathematical Foundations of Neuroscience*. Springer-Verlag, New York.
- [13] Farjami S, Kirk V, Osinga HM. Forthcoming. Computing the stable manifold of a saddle slow manifold. *SIAM Journal on Applied Dynamical Systems*.
- [14] Guckenheimer J, Holmes P. 1986. *Nonlinear Oscillations, Dynamical Systems and Bifurcations of Vector Fields*. 2nd edition. Springer-Verlag, New York.
- [15] Guckenheimer J, Krauskopf B, Osinga HM, Sandstede B. 2015. Invariant manifolds and global bifurcations. *Chaos* **25**(9):097604.
- [16] Guckenheimer J, Williams RF. 1979. Structural stability of Lorenz attractors. *Publications Mathématiques de l’Institut des Hautes Études Scientifiques* **50**(1):59–72.
- [17] Hasan CR, Krauskopf B, Osinga HM. Forthcoming. Mixed-mode oscillations and twin canard orbits in an autocatalytic chemical reaction (preprint) *SIAM Journal on Applied Dynamical Systems*.
- [18] Jackson EA. 1985. The Lorenz system: I. The global structure of its stable manifolds *Physica Scripta* **32**(5):469–475.
- [19] Jackson EA. 1985. The Lorenz system: II. The homoclinic convolution of the stable manifolds *Physica Scripta* **32**(5):476–481.
- [20] Kaplan JL, Yorke JA. 1979. Preturbulence: A regime observed in a fluid flow model of Lorenz, *Communications in Mathematical Physics* **67**:93–108.
- [21] Krauskopf B, Osinga HM. 1999. Two-dimensional global manifolds of vector fields. *Chaos* **9**(3):768–774.
- [22] Krauskopf B, Osinga HM. 2003. Computing geodesic level sets on global (un)stable manifolds of vector fields. *SIAM Journal on Applied Dynamical Systems* **2**(4):546–569.
- [23] Krauskopf B, Osinga HM. 2007. Computing invariant manifolds via the continuation of orbit segments. In Krauskopf B, Osinga HM, Galán-Vioque J, editors. *Numerical Continuation Methods for Dynamical Systems*. Springer-Verlag, New York; p. 117–154.
- [24] Krauskopf B, Osinga HM, Doedel EJ, Henderson ME, Guckenheimer J, Vladimirovsky A, Dellnitz M, Junge O. 2005. A survey of methods for computing (un)stable manifolds of vector fields. *International Journal of Bifurcation & Chaos* **15**(3):763–791.
- [25] Lorenz EN. 1963. Deterministic nonperiodic flows. *Journal of Atmospheric Science* **20**:130–141.

- [26] Mischaikow K, Mrozek M. 1995. Chaos in the Lorenz equations: A computer assisted proof, *Bulletin of the American Mathematical Society* **32**(1):66–72.
- [27] Mischaikow K, Mrozek M. 1998. Chaos in the Lorenz equations: A computer assisted proof part II: Details, *Mathematics of Computation* **67**(223):1023–1046.
- [28] Mischaikow K, Mrozek M., Szymczak A. 2001. Chaos in the Lorenz equations: A computer assisted proof part III: Classical parameter values, *Journal of Differential Equations* **169**(1):17–56.
- [29] Nowacki J, Osinga HM, Tsaneva-Atanasova KT. 2012. Dynamical systems analysis of spike-adding mechanisms in transient bursts. *The Journal of Mathematical Neuroscience* **2**:7.
- [30] Osinga HM, Krauskopf B, Hittmeyer S. 2014. Chaos and wild chaos in Lorenz-type systems. In Al-Sharawi Z, Cushing J, Elaydi S, editors. ICDEA 2013. *Theory and Applications of Difference Equations and Discrete Dynamical Systems*; May 26–30; Muscat, Oman. Springer Proceedings in Mathematics and Statistics Vol. 102. Springer-Verlag, New York; p. 75–98.
- [31] Palis J, de Melo W. 1982. *Geometric Theory of Dynamical Systems*. Springer-Verlag, New York.
- [32] Perelló C. 1979. Intertwining invariant manifolds and Lorenz attractor. In *Global Theory of Dynamical Systems*; Evanston, IL. Lecture Notes in Mathematics Vol. 819. Springer-Verlag, Berlin; p. 375–378.
- [33] Rand D. 1978. The topological classification of Lorenz attractors, *Mathematical Proceedings of the Cambridge Philosophical Society* **83**(3):451–460.
- [34] Sparrow C. 1982. *The Lorenz Equations: Bifurcations, Chaos and Strange Attractors*. Applied Mathematical Sciences Vol. 41. Springer-Verlag, New York.
- [35] Strogatz SH. 2015. *Nonlinear Dynamics and Chaos: With Applications to Physics, Biology, Chemistry, and Engineering*. 2nd edition. Westview Press, Boulder(CO)
- [36] Verhulst F. 2012. *Henri Poincaré: Impatient Genius*. Springer-Verlag, New York.